UCRL-JRNL-230312

LAWRENCE
LIVERMORE
NATIONAL
LABORATORY

Electrical Conductivity of the Lower-Mantle Ferropericlase

J. F. Lin, S. T. Weir, D. D. Jackson, W. J. Evans, Y. K. Vohra, W. Qiu, C. S. Yoo

April 27, 2007

Geophysical Research Letters

Electrical Conductivity of the Lower-Mantle Ferropericlase across the Electronic Spin Transition

Jung-Fu Lin,[1] Samuel T. Weir,[1] Damon D. Jackson,[1] William J. Evans,[1] Yogesh K. Vohra,[2] Wei Qiu,[2] and Choong-Shik Yoo[1]

[1]Lawrence Livermore National Laboratory, 7000 East Avenue, Livermore, CA 94550, USA

[2]Department of Physics, University of Alabama at Birmingham, Birmingham, AL 35124, USA

Abstract

Electrical conductivity of the lower-mantle ferropericlase-$(Mg_{0.75},Fe_{0.25})O$ has been studied using designer diamond anvils to pressures over one megabar and temperatures up to 500 K. The electrical conductivity of $(Mg_{0.75},Fe_{0.25})O$ gradually rises by an order of magnitude up to 50 GPa but decreases by a factor of approximately three between 50 to 70 GPa. This decrease in the electrical conductivity is attributed to the electronic high-spin to low-spin transition of iron in ferropericlase. That is, the electronic spin transition of iron results in a decrease in the mobility and/or density of the charge transfer carriers in the low-spin ferropericlase. The activation energy of the low-spin ferropericlase is 0.27 eV at 101 GPa, similar to that of the high-spin ferropericlase at relatively low temperatures. Our results indicate that low-spin ferropericlase exhibits lower electrical conductivity than high-spin ferropericlase, which needs to be considered in future geomagnetic models for the lower mantle. The extrapolated electrical conductivity of the low-spin ferropericlase, together with that of silicate perovskite, at the lower mantle

pressure-temperature conditions is consistent with the model electrical conductivity profile of the lower mantle.

1. Introduction

Knowledge of the electrical conductivity of the mineral assemblage in the Earth's lower mantle, mainly ferropericlase [(Mg,Fe)O] and silicate perovskite [Al-(Mg,Fe)SiO_3], is essential to understanding the propagation of the geomagnetic signals to the Earth's surface, the nature of the core-mantle coupling (e.g., Olsen, 1999; Buffet, 1992, 1996; Holme, 1998a,b), and the subtle chemistry of the deep Earth (e.g., Dobson and Brodholt, 2000a,b; Xu *et al*., 2000). Although silicate perovskite is believed to be volumetrically the dominant phase in the lower mantle, it has been demonstrated that the electrical conductivity profile of the lower mantle can be modeled with a network of ferropericlase in an insulating matrix of silicate perovskite (Wood and Nell, 1991).

The electrical conductivity of ferropericlase was previously measured up to 40 GPa and temperatures as high as ~3000 K (e.g., Mao, 1973; Peyronneau and Poirier, 1989; Li and Jeanloz, 1990; Dobson *et al*., 1997, 2000a). These studies showed that the electrical conductivity of ferropericlase is very sensitive to the iron content, ferrous to ferric iron ratio, and point defects. However, the electrical conductivity of the low-spin ferropericlase has not been measured and the potential effect of the recently observed pressure-induced electronic spin-pairing transition of iron on the electrical conductivity of ferropericlase is still unknown (e.g., Badro *et al*., 2003, Lin *et al*., 2005, 2006a,b, 2007; Speziale *et al*., 2005; Goncharov *et al*., 2006; Persson *et al*., 2006; Tsuchiya *et al*., 2006; Keppler *et al*., 2007).

Ferropericlase is a solid solution between periclase (MgO), a wide band gap insulator, and wüstite (FeO), a classical Mott insulator and an important member of the highly correlated transition metal monoxide (TMO) group (Mott, 1990; Cohen *et al.*, 1997). The Mott insulator-metal transition results from the closure of the Mott-Hubbard *d*-*d* band gap or of the charge-transfer *p*-*d* gap, and has been theoretically or experimentally reported to occur in transition metal oxides such as FeO (Cohen *et al.*, 1997; Knittle and Jeanloz, 1986), MnO (Patterson *et al*., 2004; Yoo *et al*., 2005), and Fe_2O_3 (Pasternak *et al*., 1999). In this regard, it is thus interesting to understand the effect of the electronic spin transition on the electrical conductivity of ferropercilase with iron concentration that is above the percolation threshold of 12% for the face-centered cubic (fcc) lattice, in which Fe^{2+} atoms form infinitely connected percolation path through the whole structure (Lorenz and Ziff, 1998; Lin *et al.*, 2006a).

Abnormal effects of the electronic spin transition of iron on the volume, incompressibility, sound velocities, and optical absorption spectra of ferropericlase have been observed under high pressures and room temperatures; a decrease in volume and radiative thermal conductivity and an increase in incompressibility and sound velocities are reported to occur at high pressures and room temperature (Lin *et al.*, 2005, 2006b; Speziale *et al*., 2005; Goncharov *et al.*, 2006; Keppler *et al*., 2007). These new results are changing our view of the physical and chemical states of the lower mantle. Here we have measured the electrical conductivity of ferropericlase-$(Mg_{0.75},Fe_{0.25})O$ in the diamond anvil cell (DAC) using designer diamond anvils to pressures across the spin-pairing transition and exceeding one megabar. We have also measured the temperature effect on the electrical conductivity of the low-spin ferropericlase and derived its activation energy.

2. Experiments

Polycrystalline ($Mg_{0.75}$,$Fe_{0.25}$)O was synthesized under a controlled oxygen fugacity near the iron-wüstite buffer. The sample was compositionally homogeneous in electron microprobe analyses and its ferric iron (Fe^{3+}) content was below the detection limit of Mössbauer spectroscopy. The powder sample was first compressed to ~10 GPa in a separate DAC to squeeze out voids in between grain boundaries in the sample, and then loaded into the sample chamber of 60 μm in diameter in the designer DAC (Weir *et al.*, 2000) with two beveled diamonds with an inner culet of 80 to 120 μm and an outer culet of 350 μm (Fig. 1). Tungsten electrical probes of the designer anvils were designed and fabricated at Lawrence Livermore National Laboratory, and the probes were then encased in epitaxial grown diamond layers at the University of Alabama at Birmingham (Weir *et al.*, 2000). The resistance of each tungsten probe was approximately 100 Ω whereas the probe-to-probe leakage was more than 10 GΩ. Two sets of experiments with either a six-probe or four-probe designer anvil were conducted to over one megabar. In both cases, the electrical resistance was measured using a two-probe configuration by a Keithley 6517A electrometer in the DC current. The use of the designer anvil also provided uniform and well-defined sample chamber geometry as the deformation of the sample and probe geometry can affect the resistance measurement in the DAC and complicate data interpretation (Mao *et al.*, 1973; Nellis *et al.*, 1999). We used the cell constant calculated in the three-dimensional current flow simulations (Nellis *et al.*, 1999) to relate the measured sample resistances to the electrical conductivities (Fig. 2). Conductivities obtained in this manner typically have systematic errors of up to 30% (Nellis *et al.*, 1999), due mainly to the uncertainties in the sample geometry. Our low-pressure conductivities agreed to within 50% of previously reported electrical conductivities of ferropericlase (Hansen and Cutler, 1966; Dobson *et al*., 2000a)

A small ruby sphere of 5 μm was also loaded into the sample chamber and used for pressure determination using the ruby fluorescence scale (Mao *et al*., 1978); pressures were also measured using the Raman frequency shift of the diamond first-order peak (Occelli *et al*., 2003) at above approximately 90 GPa when ruby fluorescence peaks became too weak to permit reliable pressure determination. High temperature measurements were conducted by heating the DAC with an external heater, and temperatures were measured from a K-type thermocouple attached to the diamond surface.

3. Experimental Results

The electrical conductivity of $(Mg_{0.75},Fe_{0.25})O$ has been studied up to 101 GPa and 500 K (Fig. 2) using a six-probe designer anvil. $(Mg_{0.75},Fe_{0.25})O$ remains as a semiconductor in the pressure and temperature range investigated. The electrical conductivity of $(Mg_{0.75},Fe_{0.25})O$ increases with increasing pressure by an order of magnitude up to 50 GPa, though a separate study on $(Mg_{0.78},Fe_{0.22})O$ by Mao *et al.* (1973) reported an increase of the conductivity by two orders of magnitude up to 32 GPa which was likely due to the relatively undefined sample and probe geometries. Further increase in pressure results in a decrease in the electrical conductivity of $(Mg_{0.75},Fe_{0.25})O$ by a factor of approximately three between 50 to 70 GPa (Fig. 2). The electrical conductivity then increases slightly with increasing pressure above 70 GPa. Another set of measurements to 104 GPa using a four-probe designer anvil also showed an increase in the electrical conductivity from 50 to 70 GPa by a factor of approximately two.

The electrical conductivity of the low-spin ferropericlase has also been studied at high temperatures up to 500 K at 81 GPa and 101 GPa, respectively. The measured conductivities at high temperature were fitted to the Arrhenius equation to derive the activation energy, *Ea* (Fig. 2 insert). The activation energy of the low-spin ferropericlase is 0.26 eV at 81 GPa and 0.27 eV at 101 GPa, consistent with the small polaron conduction (electronic hopping, charge transfer) (e.g., Dobson *et al.*, 1997, 2000a).

4. Discussion and Geophysical Applications

The observed decrease in the electrical conductivity between 50 to 70 GPa is consistent with the pressure range of the recently reported electronic spin-pairing transition in ferropericlase (e.g., Badro *et al*., 2003; Lin *et al.*, 2005; 2006a,b, 2007; Speziale *et al*., 2005; Goncharov *et al*., 2006; Persson *et al*., 2006; Tsuchiya *et al*., 2006; Keppler *et al*., 2007). Recent optical absorption spectra under high pressures further showed that the absorption edge of ferropericlase exhibits a red shift with increasing pressure but is shifted deeper into the ultraviolet across the spin transition above ~60 GPa. Such blue shift in the absorption edge implies a higher activation energy for the charge transfer (Gonchrov *et al*., 2006; Keppler *et al*., 2007) and is consistent with the reduced electrical conductivity of the low-spin ferropericlase observed here. That is, the electronic spin transition of iron between 50 to 70 GPa results in a decrease in the mobility and/or density of the charge transfer carriers (small polaron) in the low-spin ferropericlase, which in turn decreases the electrical conductivity across the transition.

Field observations of the electrical conductivity profile of the Earth have shown that the electrical conductivity of the Earth's lower mantle is around one to tens S/m (Olsen, 1999) whereas a highly conducting layer with the conductance of $>10^8$ S may exist at the base of the lower mantle (the exact value of conductivity depends on the thickness of the layer) (Holme, 1998a,b). Laboratory measurements of the electrical conductivity of the high-spin ferropericlase [(Mg,Fe)O] and silicate perovskite [Al-(Mg,Fe)SiO_3] under high pressures and temperatures have been used to explain the field observations (Xu *et al.*, 2000). Our results indicate that low-spin ferropericlase exhibits lower electrical conductivity than high-spin ferropericlase, which needs to be considered in future geomagnetic models for the lower mantle. High temperatures above ~1000 K may affect the conductivity mechanism in the low-spin state, because a large polaron conducting mechanism with an activation energy of 0.6 to 1 eV has been attributed to the high-temperature conductivity of the high-spin ferropericlase (Roberts *et al.*, 1995; Dobson *et al.*, 1997). It remains to be seen how the theoretically predicted spin crossover of iron in ferropericlase that extends from the middle part to the lower part of the lower mantle (Sturhahn *et al.*, 2005; Tsuchiya *et al.*, 2006; Lin *et al.*, 2007) affect the electrical conductivity of ferropericlase as well as silicate perovskite at the lower mantle pressure-temperature conditions.

An extrapolation of the electrical conductivity of the low-spin ferropericlase to the lower-mantle pressure-temperature conditions yields an electrical conductivity in the order of tens of S/m, consistent with the model values for the lower mantle (e.g., Olsen, 1999). Such value is apparently too low to account for the possible existence of a highly conducting layer with the conductance of $>10^8$ S at the base of the lower mantle (the conductivity depends on the thickness of the layer) (Holme, 1998a,b), though possible existence of metallic FeO and addition of ferrous iron can significantly alter the conductivity of the region (Knittle and Jeanloz, 1986; Cohen *et al.*, 1997; Dobson and Brodholt, 2005). Alternatively, a highly conducting post-perovskite phase existing at the core-mantle boundary (Ono *et al.*, 2006) has been invoked to explain the exchange of the angular momentum and electromagnetic coupling between the liquid core and the solid mantle that result in the observed changes in the Earth's length of day (e.g., Buffet, 1992, 1996; Holmes, 1998a,b). However, the electrical conductivity of the post-perovskite phase is unknown and is only suggested to be much larger than the perovskite phase based on the analogous transition in Al_2O_3 (Ono *et al.*, 2006) that results in a two order of magnitude increase in the conductivity above 200 GPa (Weir *et al.*, 1996). Future studies on the electrical conductivities of FeO and post-perovskite phase using our novel designer anvil technique with well fabricated electrical probes will help in understanding their potential roles in the geomagnetism at the core-mantle region.

Acknowledgments. This work at LLNL was performed under the auspices of the U.S. DOE by University of California and LLNL under Contract No. W-7405-Eng-48. We thank J. Roberts, R. Cohen, R. Wentzcovitch, D. Dobson, W. Sturhahn, and G. Shen for helpful discussion and S. D. Jacobsen for his help with the sample synthesis. We also acknowledge H. Keppler for sharing his manuscript with us. J.F.L. is also supported by the Lawrence Livermore Fellowship.

References

Badro, J. *et al.*, Iron partitioning in Earth's mantle: toward a deep lower mantle discontinuity, *Science*, *300*, 789-791, 2003.

Buffett, B. A., Constraints on magnetic energy and mantle conductivity from the forced nutations of the Earth, *J. Geophys. Res.*, *97*, 19581–19597, 1992.

Buffett, B. A., A mechanism for decade fluctuations in the length of day, *Geophys. Res. Lett.*, *23*, 3803–3806, 1996.

Cohen, R. E., I. I. Mazin, and D. G. Isaak, Magnetic collapse in transition metal oxides at high pressure: implications for the Earth, *Science*, *275*, 654-657, 1997.

Dobson, D. P., N. C. Richmond, and J. P. Brodholt, A high-temperature electrical conduction mechanism in the lower mantle phase $(Mg,Fe)_{1-X}O$, *Science*, *275*, 1779-1781, 1997.

Dobson, D. P., and J. P. Brodholt, The electrical conductivity of the lower mantle phase magnesiowüstite at high temperatures and pressures, *J. Geophys. Res.*, *105*, 531-538, 2000a.

Dobson, D. P., and J. P. Brodholt, The electrical conductivity and thermal profile of the Earth's mid-mantle, *Geophys. Res. Lett.*, *27*, 2325-2328, 2000b.

Dobson, D. P., and J. P. Brodholt, Subducted banded iron formations as a source of ultralow-velocity zones at the core–mantle boundary, *Nature*, *434*, 371-374, 2005.

Goncharov, A. F., V. V. Struzhkin, and S. D. Jacobsen, Reduced radiative conductivity of low-spin (Mg,Fe)O in the lower mantle, *Science*, *312*, 1205-1208, 2006.

Hansen, K. W., and I. B. Cutler, Electrical conductivity in $Fe_{1-X}O$-MgO solid solutions, *J. Am. Ceram. Soc.*, *49*, 100-102, 1966.

Holme, R., Electromagnetic core–mantle coupling, I, explaining decadal changes in the length of day, *Geophys. J. Int.*, *132*, 167–180, 1998a.

Holme, R., Electromagnetic core–mantle coupling: II. Probing deep mantle conductance, in: M. Gurnis, M.E. Wysession, E. Knittle, B.A. Buffett (Eds.), The Core–Mantle Boundary Region, AGU, pp. 139–151, 1998b.

Keppler, H., I. Kantor, and L. S. Dubrovinsky, Optical absorption spectra of ferropericlase to 84 GPa, *Am. Miner*. (in press), 2007.

Knittle, E., and R. Jeanloz, High-pressure metallization of FeO and implications for the Earth's core, *Geophys. Res. Lett.*, *13*, 1541-1544, 1986.

Li, X., and R. Jeanloz, High pressure-temperature electrical conductivity of magnesiowüstite as a function of iron oxide concentration, *J. Geophys. Res.*, *95*, 21609-21612, 1990.

Lin, J. F. *et al.*, Spin transition of iron in magnesiowüstite in Earth's lower mantle, *Nature*, *436*, 377-380, 2005.

Lin**,** J. F. *et al*., Pressure-induced electronic spin transition of iron in magnesiowüstite-(Mg,Fe)O, *Phys. Rev. B*, *73*, 113107, 2006a.

Lin, J. F. *et al*., Sound velocities of ferropericlase in the Earth's lower mantle, *Geophys. Res. Lett.*, **33**, L22304, doi:10.1029/2006GL028099, 2006b.

Lin, J. F., S. D. Jacobsen, and R. M. Wentzcovitch, Electronic spin transition of iron in the Earth's deep mantle, *Eos. Trans. American Geophysical Union, 88*, 2, pages 13,17, 2007.

Lorenz, C. D., and R. M. Ziff, Precise determination of the bond percolation thresholds and finite-size scaling corrections for the sc, fcc, and bcc lattices, *Phys. Rev. E*, *57*, 230-236, 1998.

Mao, H. K., Observations of optical absorption and electrical conductivity in magnesiowüstite at high pressures, *Carnegie Inst. Washington Yearb.*, *72*, 554-557, 1973.

Mao, H. K., P. M. Bell, J. W. Shaner, and D. J. Steinberg, Specific volume measurements of Cu, Mo, Pd, and Ag and calibration of the ruby R_1 fluorescence pressure gauge from 0.06 to 1 Mbar, *J. Appl. Phys.*, *49*, 3276-3283, 1978.

Mott, M. F., Metal Insulator Transitions, 2nd ed., 286 pp., Tayor and Francis, London, 1990.

Nellis, W., S. Weir, and A. Mitchell, Minimum metallic conductivity of fluid hydrogen at 140 GPa (1.4 Mbar), *Phys. Rev. B*, *59*, 3434-3449, 1999.

Occelli, F., P. Loubeyre, and R. Letoullec, Properties of diamond under hydrostatic pressures up to 140 GPa, *Nat. Mater.*, *2*, 151-154, 2003.

Olsen, N., Long-period (30 days-1 year) electromagnetic sounding and the electrical conductivity of the lower amntle beneath Europe, *Geophys. J. Int.*, *138*, 179-187, 1999.

Ono, S., A. R. Oganov, T. Koyama, and H. Shimizu, Stability and compressibility of the high-pressure phases of Al_2O_3 up to 200 GPa: Implications for the electrical conductivity of the base of the lower mantle, *Earth Planet. Sci. Lett.*, *246*, 326–335, 2006.

Pasternak M. P. *et al.*, Breakdown of the Mott-Hubbard state in Fe_2O_3: A first-order insulator-metal transition with collapse of magnetism at 50 GPa, *Phys. Rev. Lett.*, *82*, 4663-4666, 1999.

Patterson, J. R. *et al.*, Pressure-induced metallization of the Mott insulator MnO, *Phys. Rev. B*, *69*, 220101(R), 2004.

Persson, K., Bengtson, A., Ceder, G., & Morgan, D. *Ab initio* study of the composition dependence of the pressure-induced spin transition in the $(Mg_{1-x},Fe_x)O$ system, *Geophys. Res. Lett., 33*, L16306, 2006.

Peyronneau, J., and J. P. Poirier, Electrical conductivity of the Earth's lower mantle, *Nature*, *342*, 537-539, 1989.

Roberts, J., *et al*., Electrical properties of $Mg_{0.83}Fe_{0.17}O$ in a gas mixing furnace and the diamond anvil cell, *Eos, 76*, S156, 1995.

Tsuchiya, T., R. M. Wentzcovitch, C. R. S. da Silva, and S. de Gironcoli, Spin transition in magnesiowüstite in Earth's lower mantle, *Phys. Rev. Lett.*, *96*, 198501, 2006.

Speziale, S. *et al*., Iron spin transition in Earth's mantle, *Proc. Natl. Acad. Sci. USA, 102*, 17918-17922, 2005.

Sturhahn, W., J. M. Jackson, and J. F. Lin, The spin state of iron in Earth's lower mantle minerals, *Geophys. Res. Lett.*, *32*, L12307, 2005.

Weir, S. T., A. C. Mitchell, and W. J. Nellis, Electrical resistivity of single-crystal Al_2O_3 shock-compressed in the pressure range 91–220 GPa (0.91–2.20 Mbar), *J. Appl. Phys.*, *80*, 1522–1525, 1996.

Weir, S. T., J. Akella, C. Aracne-Ruddle, Y. K. Vohra, and S. A. Catledge, Epitaxial diamond encapsulation of metal microprobes for high pressure experiments, *Appl. Phys. Lett.*, *77*, 3400-3402, 2000.

Wood, B. J., and J. Nell, High-temperature electrical conductivity of the lower-mantle phase (Mg,Fe)O, *Nature*, *351*, 309-311, 1991.

Xu, Y., T. J. Shankland, and B. T. Poe, Laboratory-based electrical conductivity in the Earth's mantle, *J. Geophys. Res.*, *105*, 27865–27875, 2000.

Yoo, C. S. *et al.* First-Order Isostructural Mott Transition in MnO, *Phys. Rev. Lett.*, *94*, 115502, 2005.

Figure Captions

Figure 1. (a). Image of a designer diamond anvil with six tungsten probes used in the high-pressure electrical conductivity experiments (in both transmitted and reflected lights). The beveled anvil has an inner culet of 120 μm and an outer culet of 350 μm. The microprobes were made of thin-film tungsten ~15 μm wide and ~0.5 μm thick, and were covered by the epitaxial deposited diamond except small contact areas emerging from the synthetic diamond layer. (b). $(Mg_{0.75},Fe_{0.25})O$ sample in a DAC at 81 GPa (in reflected light). Re was used as the metal gasket to confine the sample of 60 μm in diameter. The sample was opaque to the transmitted light and showed dull reflection to the white light.

Figure 2. Electrical conductivities of $(Mg_{0.75},Fe_{0.25})O$ as a function of pressure obtained from a six-probe designer anvil cell. The conductivity increases by an order of magnitude up to 50 GPa but drops by a factor of approximately three from 50 to 70 GPa. Dotted line: electrical conductivities of $(Mg_{0.78},Fe_{0.22})O$ at high pressures (Mao, 1973). Insert, electrical conductivities of $(Mg_{0.75},Fe_{0.25})O$ plotted against absolute reciprocal temperature at 101 GPa. Open circles: experimental data; solid line: fit to the Ahrrenius equation.

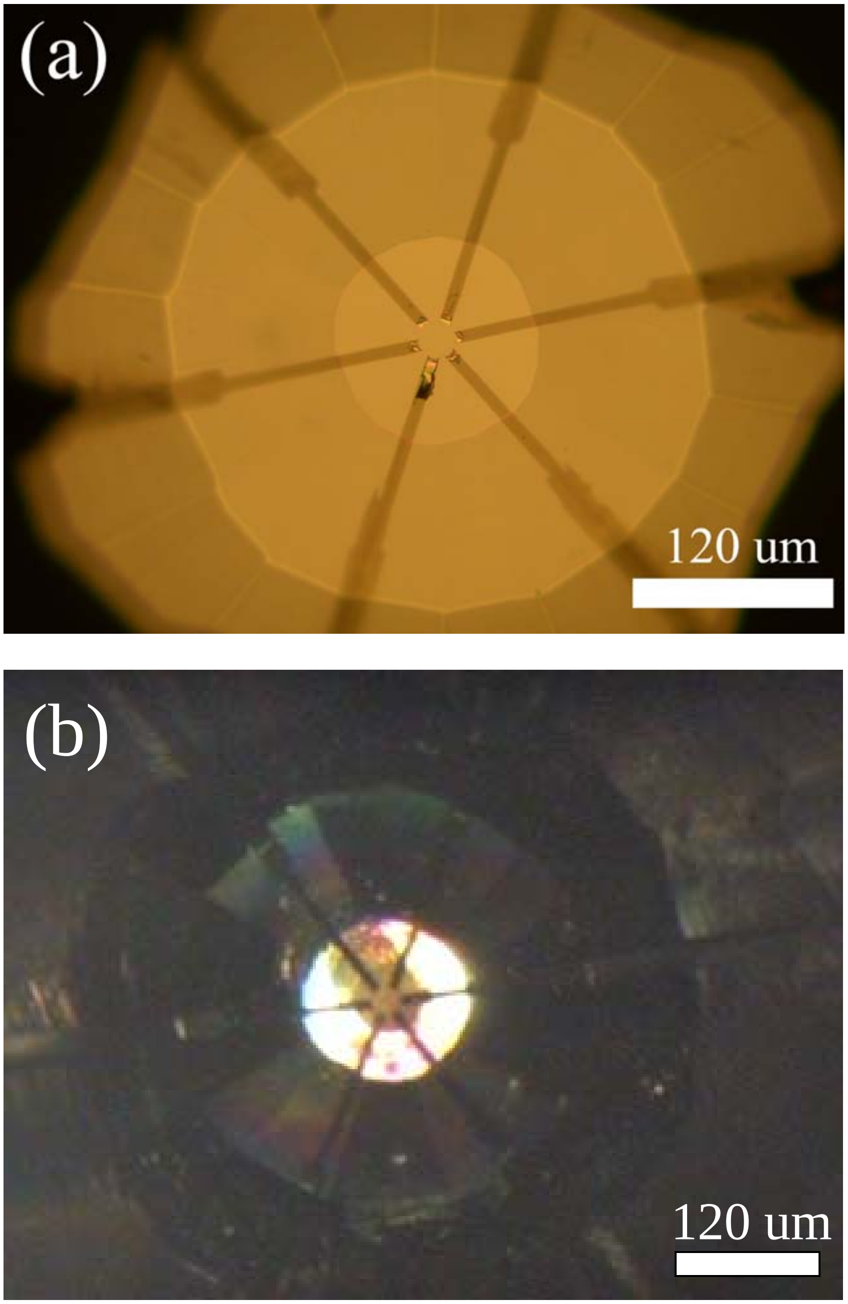
(a)
120 um
(b)
120 um

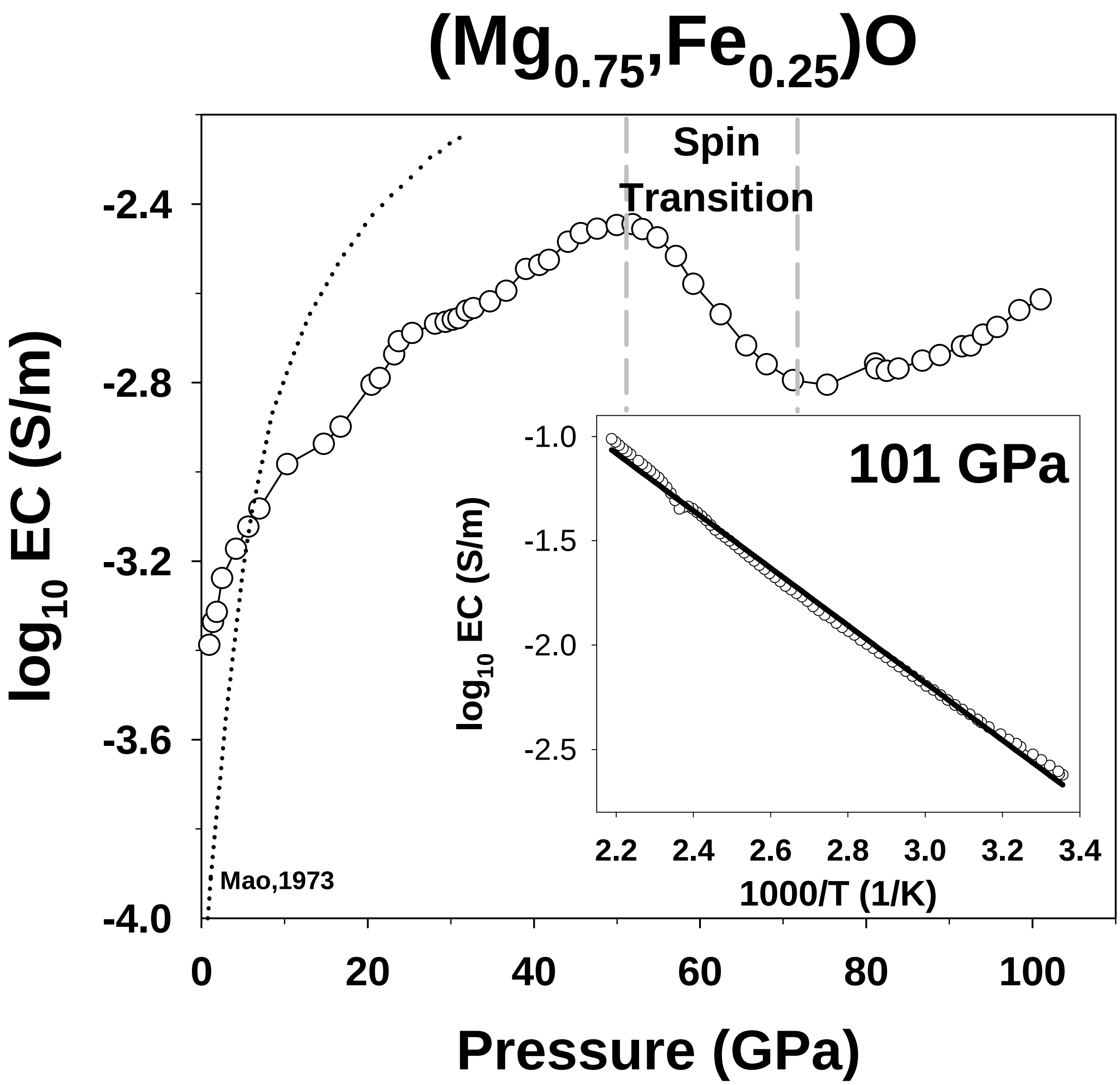

(Mg0.75,Fe0.25)O
Spin
Transition
101 GPa
log10 EC (S/m)
-2.4
-2.8
-3.2
-3.6
-4.0
0
20
40
60
80
100
Pressure (GPa)
Mao,1973
-1.0
-1.5
-2.0
-2.5
2.2
2.4
2.6
2.8
3.0
3.2
3.4
1000/T (1/K)

Fig. 2